Int. J. Advanced Design and Manufacturing Technology, 2025, Vol. 18, No. 3, pp. 43-49

DOI: *ISSN: 2252-0406* *https://admt.isfahan.iau.ir*

Experimental Study of Magnetic Field-Aided Friction Stir Spot Welding

Farshad Akbari, Seyed Mohammad Hossein Seyedkashi *
Department of Mechanical Engineering,
University of Birjand, Iran
E-mail: Farshad2773@gmail.com, seyedkashi@birjand.ac.ir
*Corresponding author

Moosa Sajed
Department of Mechanical Engineering,
Azarbaijan Shahid Madani University, Iran
E-mail: sajed@azaruniv.ac.ir

Received: 19 April 2025, Revised: 20 May 2025, Accepted: 1 November 2025

Abstract: Magnetic field is applied during the friction stir spot welding of St37 steel to achieve a better microstructure and mechanical properties. The process is called magnetic field-aided friction stir spot welding. The magnetic field is applied using an induction heater module and coil in which the welding tool acts as the core for the coil. The effects of tool rotational speed, voltage, and dwell time on the strength and microstructure of welded samples are investigated. The strength of joints increased using a magnetic field, and the effect is stronger when a lower tool rotational speed and dwell time are used. This could be attributed to the heat input by applying the Eddy current in the nugget together with a finer microstructure, which is achieved by applying the magnetic field. The increase of all three parameters simultaneously overheats the nugget and results in a drop in the strength of the joint. The highest strength of 5159.5 N is achieved with a tool rotational speed, a dwell time, and a voltage of 2000 rpm, 6 s, and 25 V, respectively.

Keywords: Friction Stir Spot Welding, Magnetic Field, Magnetic Field Aided Friction Stir Spot Welding, Mechanical Properties,

Biographical notes: Farshad Akbari received his BSc and MSc in Manufacturing Engineering from the Technical and Vocational University in 2016 and the University of Birjand in 2021, respectively. His research interest is friction stir welding process. **Seyed Mohammad Hossein Seyedkashi** received his PhD degree (Manufacturing Engineering) from Tarbiat Modares University in 2012. He is currently a professor in the Department of Mechanical Engineering, University of Birjand, Birjand, Iran. His research interests are sheet metal forming, friction stir welding, additive manufacturing and optimization. **Moosa Sajed** is an Assistant Professor at Azarbaijan Shahid Madani University. He received his PhD in Manufacturing Engineering from the University of Birjand in 2021. His research interests include solid-state processing, mechanical alloying, and finite element analysis.

Research paper

1 INTRODUCTION

Friction Stir Welding (FSW) was invented in 1991 by The Welding Institute (TWI) [1]. It is a solid-state and environmentally friendly welding process that can be used to join high-strength aluminum alloys and those that cannot be welded by conventional welding processes. In the process, a non-consumable rotary tool that contains a pin and shoulder penetrates the interface of two plates to be welded [2]. The tool has two main roles: heat production and material movement. The produced frictional heat makes the material soft enough that it is then stirred by a rotary pin [3]. Tool feed rate, tool rotational speed, and axial load are the main process parameters [4]. The tool pin profile is also an important parameter. The main pin profiles are square, triangle, threaded, and simple cylinder [5].

Friction stir spot welding is a variant of the main process, where there is no transverse movement of the tool, and joining occurs in a small zone. Research has been performed to increase the strength of the joint. For example, Venukumar et al. [6] investigated the strength and fatigue behavior of refilled friction stir spot welded 6061 aluminum sheets. They used a tool with a retractable pin to join and refill the spot weld. They reported an increase in the strength of the joint by refilling, but no change in the fatigue behaviour of the joints. Sajed [7] introduced two-stage refilled friction stir spot welding to refill the keyhole simply. He mentioned the pinless tool shoulder diameter as the most effective parameter on the weld strength. The exact process was used by Akbari et al. [8] to join polyethylene sheets. They reported higher strength at a lower tool rotational speed.

The application of a magnetic field in the welding zone is a common technique used to increase joint strength and achieve a fine microstructure. Mou et al. [9] reported that electric and magnetic fields can improve the joint microstructure in cold metal transfer. The Lorentz force makes the arc move in a circular path. It also shortens the arc length and widens its width. They reported an increase in the joint strength from 270.7 to 387.8 MPa as a result of using a magnetic field. Liu et al. [10] applied a magnetic field during the welding of copper sheets. They reported that the thickness of the Al_2Cu inter-metallic decreased from 50 to 5 μm as a result of the application of the magnetic field. They also reported an increase in the strength of the joint. Sun et al. [11] reported magnetic field-aided CMT welding of Al6061-T6 and TC4 alloys. They concluded that the magnetic field increases the transmission ability of the fusion pool. Cao et al. [12] investigated the effect of the magnetic field on the welding nugget in laser welding of aluminum alloys. They reported that the Lorentz force is applied by the magnetic field in the opposite direction of the fusion pool, which restricts the width of grains. Chen et al. [13] investigated the magnetic field-assisted welding of steel. According to the results, the ultimate strength was increased by 43.9% and the grains were finer by a factor of 2.

In the present paper, a magnetic field is applied during the friction stir spot welding of St37 steel sheets and its effect is investigated on the strength and microstructure of the joints. A setup was designed to apply the magnetic field to the welding zone, including a transformer, induction heater module, cooling system, and a coil. The welding tool acts as a core for the coil during the welding, and an Eddy current is induced that heats the nugget. However, the presence of the magnetic field restricts the grain growth, and a finer microstructure could be achieved so that the heat is induced on the nugget with no grain growth.

The main innovation of the present paper is applying a magnetic field concurrently with friction stir spot welding of low-carbon steel sheets. Friction stir welding is successfully applied to a wide range of engineering materials, from polymers to alloys. When welding high strength alloys is the case, using auxiliary energies is a standard method. Electrical current is a widely adopted heating source that is used in this case. However, what is considered in this paper is applying a magnetic field during the welding process, which was not carried out before, to the best of the authors' knowledge. This field prevents grains from growing considerably, which makes the joints stronger.

2 MATERIAL AND METHODS

St37 steel sheets with dimensions of 1×50×160 mm3 were used to carry out the experiments. The chemical composition of St37 alloy is presented in “Table 1”.

Table 1 The chemical composition of St37 steel [14]

C	Si	Mn	P	S	Cr	Ni	Fe
0.11	0.03	0.56	0.007	0.005	0.07	0.03	Bal.

In this process, frequency is applied using an induction heater module driven by a transformer with a current of 20 A. The induction heater is an electric device that produces heat by inducing a magnetic field. A wire with a diameter of 2 mm was used to fabricate a coil with 9 loops and an internal diameter of 30 mm. The coil that is connected to the induction heater is used to transfer the produced frequency. Figure 1 presents the induction heater module, its fixture, the cooling system, and the coil.

The produced magnetic field is transmitted to the coil, which creates a current that varies with time according to Faraday’s Law, known as the Eddy current. The

Eddy currents flow through the workpiece in closed circles. The direction of the currents is orthogonal to the magnetic field. The amount of the Eddy current is directly dependent on the magnetic field, area of the ring, and magnetic flux variation, while it varies inversely with any variations in the conduction of the wire. Figure 2 presents the Eddy current in the workpiece.

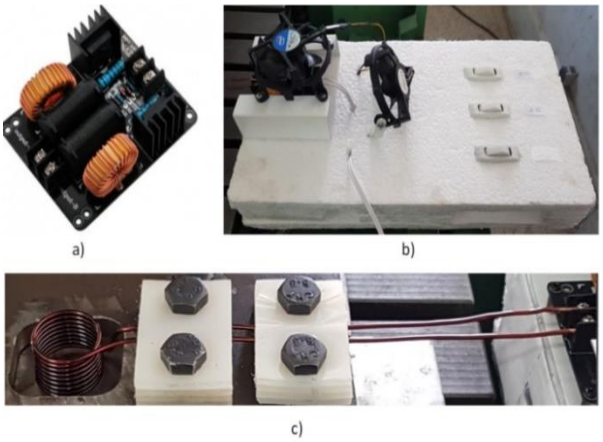

Fig. 1 (a): The induction heater module, (b): the fixture of the induction heater and cooling system, and (c): the coil.

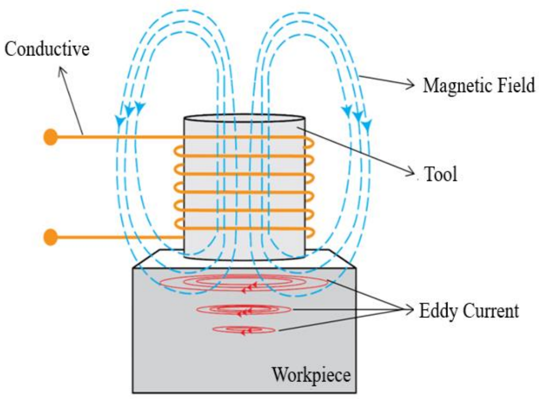

Fig. 2 Eddy current in the workpiece.

The experiments were carried out using a universal CNC FP4M milling machine. The tool material was WC. Figure 3 presents the tool and a typical welded sample, along with their dimensions. The experiment setup is also illustrated in "Fig. 4". The tool rotational speed, dwell time, and voltage were investigated as key parameters. Three levels were considered for all parameters. The full factorial design of experiments was considered, and 27 test sets were obtained. The levels of investigated parameters are summarized in "Table 2".

To evaluate the effects of input parameters on the strength and microstructure of the joints, the tensile-shear test was carried out, and the microstructure of the joints was evaluated using an optical microscope. The results of the tensile-shear test, together with process parameters corresponding to each experiment, are given in "Table 3".

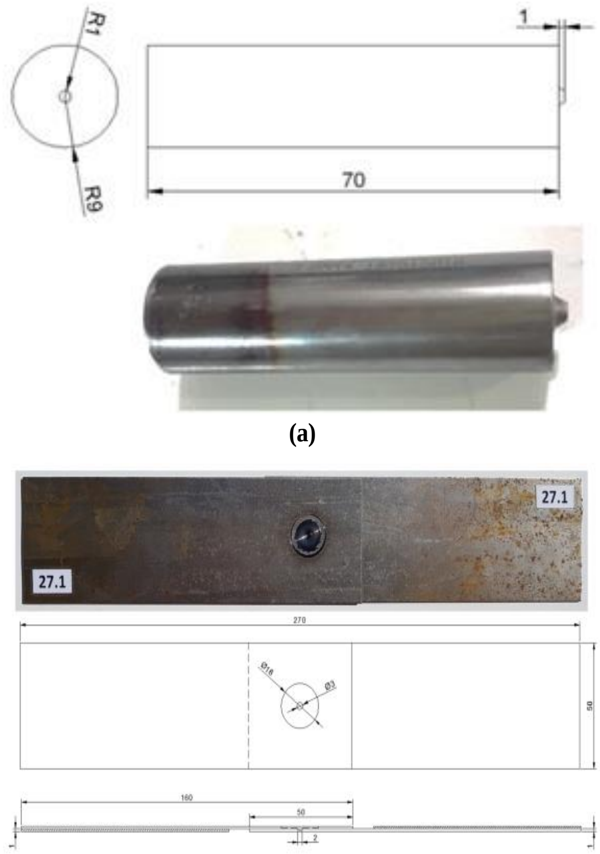

(b)

Fig. 3 (a): The tool and its dimensions, and (b): a typical welded sample and its dimensions.

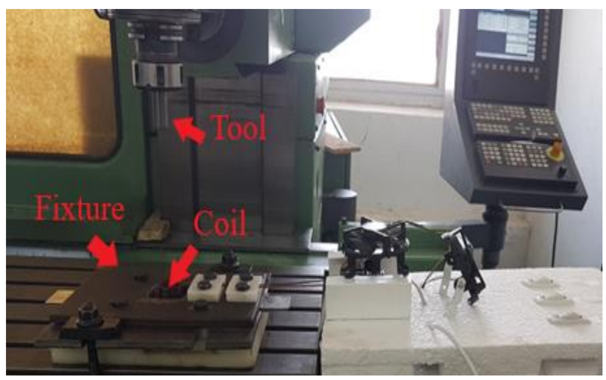

Fig. 4 The experiment setup.

Table 2 The investigated parameters and their levels

Levels	Rotational Speed (rpm)	Dwell Time (s)	Voltage (V)
1	1000	3	0
2	1500	6	18
3	2000	9	25

Table 3 The parameters of experiments and results of the tensile-shear test

No.	Tool Rotational Speed (rpm)	Dwell Time (s)	Voltage (V)	Tensile-Shear Strength (N)
1	1000	3	0	405.6
2	2000	3	18	2576.6
3	1000	9	18	2775.2
4	1500	6	25	4055.1
5	2000	6	18	4860.2
6	2000	6	25	5159.5
7	1500	9	18	4116.4
8	1500	3	0	849.2
9	1000	9	25	3181.6
10	1000	3	18	1248.8
11	2000	6	0	4666.5
12	2000	9	0	4352.5
13	1000	6	18	1550.2
14	2000	3	0	1168.4
15	1500	3	25	2353.2
16	1000	6	0	1501.7
17	1000	6	25	2191.9
18	2000	9	18	3829.8
19	1500	6	0	1843.1
20	1000	9	0	2897.3
21	1500	9	0	3276.7
22	1000	3	25	1234.8
23	2000	3	25	3525.0
24	1500	6	18	3470.2
25	1500	3	18	1933.8
26	1500	9	25	3513.7
27	2000	9	25	3562.2

3 RESULTS AND DISCUSSION

Generally, the heat generation and propagation pattern, as well as the temperature level, are key factors that determine the joint quality in friction-based processes [15]. When steel is welded using friction stir welding, it is essential to provide enough heat input in the welding nugget to achieve a sound weld. Thus, using auxiliary heat sources could be helpful. In this research, a magnetic field was applied during the welding to study the effect of Eddy current on the strength and microstructure of spot joints in St37 sheets. Tool rotational speed and dwell time as the main sources of heat input in welding were also investigated.

"Table 4" presents the results of the analysis of variance for the strength of joints. According to the results, dwell time, with a contribution percentage of 38.08%, is the most effective input parameter, followed by tool rotational speed and voltage, with contribution percentages of 34.41% and 7.89%, respectively. When 2-way interactions are considered, the interaction of tool rotational speed and dwell time has the maximum contribution on the joint strength, with a contribution percentage of 9.08% followed by the voltage and dwell time interaction and the interaction of voltage and tool rotational speed, with contribution percentages of 5.08% and 1.89%, respectively. The main effects plot is presented in "Fig. 5". The strength increases by increasing all three investigated parameters. However, it is sharper in the case of dwell time. Any increases in any of the investigated parameters increase the amount of heat input in the welding nugget, which can be considered a reason for the same trends observed in the main plots.

Table 4 Analysis of Variance for the strength of joints

Source	DF	Seq SS	Contribute	P-Value
Model	18	43485158	96.41%	0.001
Linear	6	36252665	80.38%	0.000
Voltage	2	3558754	7.89%	0.010
Rotational Speed	2	15519115	34.41%	0.000
Dwell Time	2	17174796	38.08%	0.000
2-Way Interactions	12	7232493	16.04%	0.065
Voltage×Rotational Speed	4	850199	1.89%	0.439
Voltage×Dwell Time	4	2289072	5.08%	0.098
Rotational Speed×Dwell T	4	4093222	9.08%	0.025
Error	8	1617571	3.59%	
Total	26	45102729	100.00%	

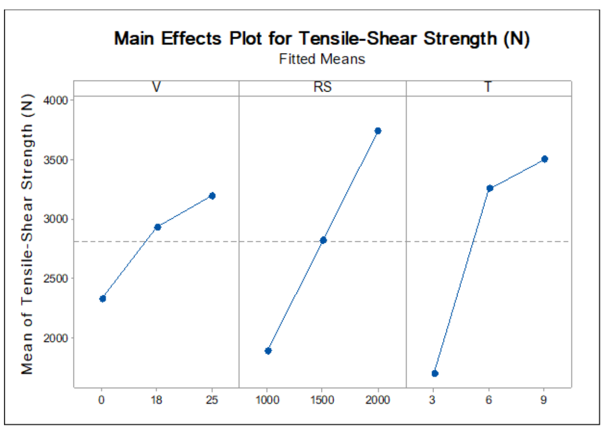

Fig. 5 The main effects plot (V=voltage, RS=tool rotational speed, and T=dwell time).

Increasing the dwell time from 3 to 6 s, makes a significant increase in the strength of the joint, while further growing dwell time from 6 to 9 s does not considerably affect the strength. This indicates that when the dwell time is less than 6 seconds, there is insufficient time for the material to be mixed properly. Also, further increase in the time is not necessary when the welding sheets are low carbon steels. However, for tool rotational speed, any increase from 1000 to 2000 rpm increases the joint strength considerably. The plot indicates that using tool rotational speeds more than 2000 rpm, may result in even stronger joints. This should be investigated in future studies. The effect of increasing the voltage is just like increasing the tool rotational speed. However, it is less effective on joint strength when compared to the tool rotational speed. The interaction plots are also presented in “Fig. 6”.

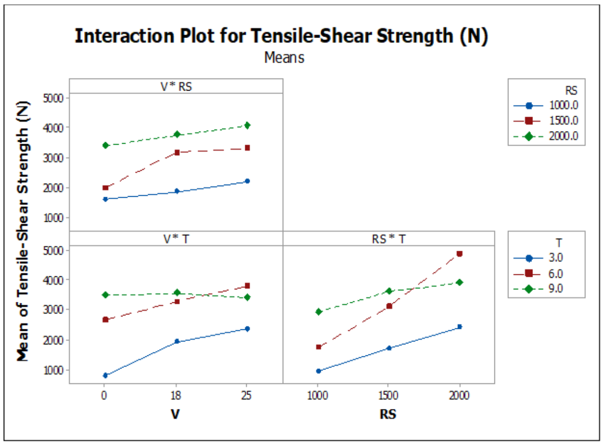

Fig. 6 The interaction plots (V=voltage, RS=tool rotational speed, and T=dwell time).

According to “Fig. 6”, the interaction of tool rotational speed and voltage can be ignored due to the semiparallel plot of that. On the other hand, when the voltage is at its highest level, i.e. 25V, increasing dwell time from 6 to 9s results in a drop in strength of the joint, which can be attributed to the overheating of the nugget and the resulting grain growth [16]. The same effect is detectable when the tool rotational speed is at its fastest level, i.e. 2000 rpm, and dwell time increases from 6 to 9s. Thus, it could be concluded that although a higher dwell time is needed when steel is welded, overall heat input to the welding nugget should be considered, and an optimal set of parameters should be applied based on it.

According to the results, welding parameters, including tool rotational speed and dwell time, are much more significant on the strength of joints in comparison to the voltage in both main and interactive effects. However, according to “Table 3”, when the tool rotational speed is at its lowest level, i.e. 1000 rpm, a comparison between the strength of welded samples presents a significant effect of the application of the magnetic field. The strength is just 405.6 N for sample 1 which was welded with a tool rotational speed of 1000 rpm, dwell time of 3s, and no voltage, while it is 1248.8 and 1234.8 N for samples 10 and 22, respectively, which were welded with the same rotational speed and dwell time but with a voltage of 18 and 25 V, respectively. This indicates that the strength of the joint was almost tripled when the magnetic field was applied. Thus, it could be concluded that heat input is a key factor when steel sheets are spot-welded, and the main sources of heat input are tool rotational speed and dwell time. However, when a lower tool rotational speed is needed, a magnetic field could be introduced to the nugget to increase the joint strength. On the other hand, the main disadvantage of the friction stir spot welding in comparison with resistance welding, when it is applied on steel, is the time of the process. Using a magnetic field during the friction stir spot welding, one can reduce the dwell time without a significant drop in strength to make the process more favorable and faster.

Four distinct areas presented in “Fig. 7” could be determined in the microstructure of friction stir spot welded joints; stir zone (SZ), thermo-mechanically affected zone (TMAZ), heat affected zone (HAZ), and base metal (BM) [17].

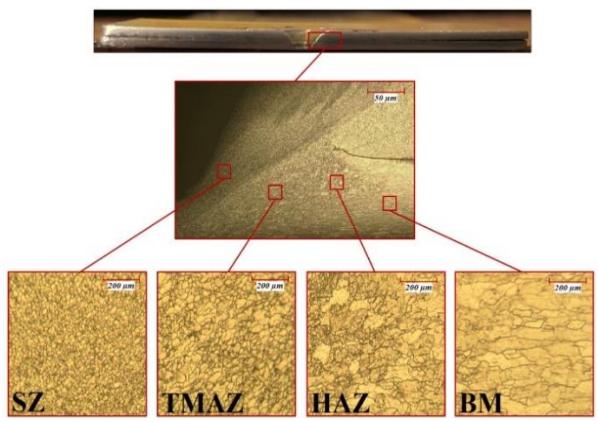

Fig. 7 Microstructural zones with a tool rotational speed of 2000 rpm, dwell time of 9s, and voltage of 25V.

In samples welded at a lower tool rotational speed and dwell time, it is evident that there was no proper stirring during the welding process, which could be attributed to the lower heat input. In these samples, improper joints, cracks, and porosity were detected in the microstructure of the joint. Better stirring is evident when a longer dwell time is used, providing more time for stirring together with a higher heat input. The tool's rotational speed can be considered the main parameter affecting heat generation during welding. Generally, any increase in the tool rotational speed results in a higher strain rate and more plastic deformation [18].

Any increase in the tool rotational speed also widens the microstructural zones, which is evident in "Fig. 8" where defects are pointed by arrows.

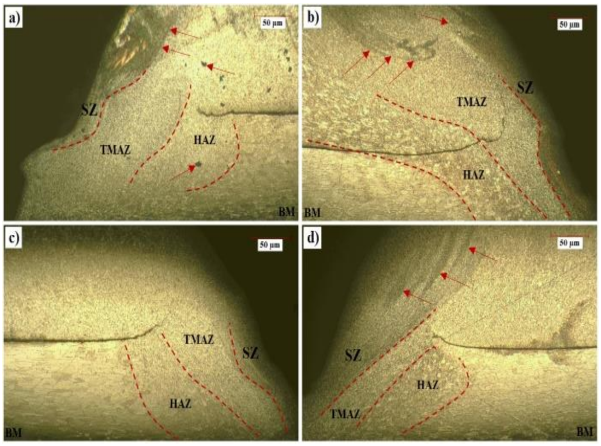

Fig. 8 Microstructural zones in the samples without the magnetic field and with tool rotational speed and dwell time of: (a): 1000 rpm and 3s, (b): 1000 rpm and 9s, (c): 2000 rpm and 3s, and (d): 2000 rpm and 9s. Arrows point to the defects.

In the TMAZ, there is not enough driving force for dynamic recrystallization because the strain rate and temperature are lower compared to the stir zone [19]. According to "Fig. 8", there are coarse grains together with defects in this zone when a lower tool rotational speed is used. An increase in the tool rotational speed results in a fine microstructure, and also the defects vanish.

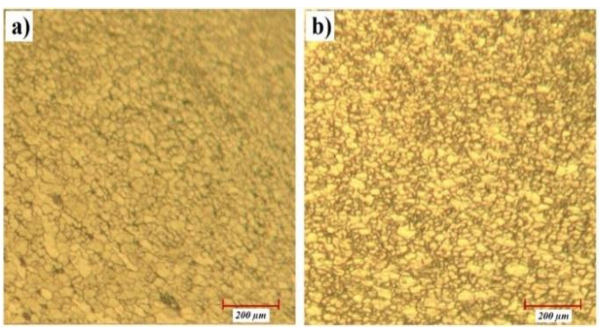

Fig. 9 Stir zone of the sample welded with a tool rotational speed, dwell time, and voltage of: (a): 1500 rpm, 6s, 0V, and (b): 1500 rpm, 6s, and 25 V.

In the case of higher heat input, two failure mechanisms are detectable, including the formation of intermetallic compounds (mostly in welding of dissimilar alloys) and the onset of defects [20]. In this study, any increase in parameters results in higher heat input in the welding nugget. Thus, the joint strength does not have its highest value when the highest levels of all parameters are used (see "Table 3"). Application of a magnetic field results in fine grains when a lower tool rotational speed and dwell time are used (see "Fig. 9") and also a bigger stir zone. However, more defects are present when these parameters are at their highest level, leading to a lower joint strength.

4 CONCLUSIONS

In this paper, magnetic field-aided friction stir spot welding of St37 steel was conducted. Three input parameters, including tool rotational speed, dwell time, and voltage, were investigated. The strength of joints was evaluated, and the microstructure of welding nuggets was also investigated. The main results are as follows:

- Any increase in the tool rotational speed, dwell time, and voltage results in an increase in the strength of the joint due to more heat input.
- The stirring is not enough when a lower tool rotational and dwell time are used, and proper joining does not take place in this case.
- Application of a magnetic field results in a bigger stir zone and finer microstructure, and then stronger joints. This effect is stronger when a lower tool rotational speed and dwell time are used.
- The welding nugget is overheated when all parameters are in their highest levels, which results in defect formation, a coarse microstructure, and hence a reduction in the joint strength.
- The best strength was 5159.5 N, which was achieved by sample 6, which was welded with a tool rotational speed, dwell time, and voltage of 2000 rpm, 6s, and 25V, respectively.

REFERENCES

[1] Thomas, W. M., Nicholas, E. D., Needham, J. C., and et al., Friction Welding, USA Patent No. US5460317A, 1995.

[2] Sattari, S., Bisadi, H., and Sajed, M., Mechanical Properties and Temperature Distributions of Thin Friction Stir Welded Sheets of AA5083, International Journal of Mechanics and Applications, Vol. 2, No. 1, 2012, pp. 1-6.

[3] Sajed, M., Bisadi, H., Experimental Failure Study of Friction Stir Spot Welded Similar and Dissimilar Aluminum Alloys, Welding in the World, Vol. 60, No. 1, 2016, pp. 33-40.

[4] Paidar, M., Khodabandeh, A., Lali Sarab, M., and et al., Effect of Welding Parameters (Plunge Depths of Shoulder, Pin Geometry, and Tool Rotational Speed) on the Failure Mode and Stir Zone Characteristics of Friction Stir Spot Welded Aluminum 2024-T3 Sheets, Journal of Mechanical Science and Technology, Vol. 29, 2015, pp. 4639-4644.

[5] Atak, A., Impact of Pinless Stirring Tools with Different Shoulder Profile Designs on Friction Stir Spot Welded

Joints, Journal of Mechanical Science and Technology, Vol. 34, 2020, pp. 3735-3743.

[6] Venukumar, S., Yalagi, S., and Muthukumaran, S., Comparison of Microstructure and Mechanical Properties of Conventional and Refilled Friction Stir Spot Welds in AA 6061-T6 Using Filler Plate. Transactions of Nonferrous Metals Society of China, Vol. 23, No. 10, 2013, pp. 2833-2842.

[7] Sajed, M., Parametric Study of Two-Stage Refilled Friction Stir Spot Welding, Journal of Manufacturing Processes, Vol. 24, 2016, pp. 307-317.

[8] Akbari, F., Sajed, M., Ashrafi, A., and Seyedkashi, S. M. H., Influence of Welding Parameters on Strength of Friction Stir Spot Welded Polyethylene Sheets Using Two-Stage Refilling Process, Proceedings of the 4th International Conference on Manufacturing Engineering, 2018.

[9] Mou, G., Hua, X., Wang, M., and et al., Effect of Axial Magnetic Field on Cold Metal Transfer Arc-Brazing of Ti6Al4V to 304L Steel. Journal of Materials Processing Technology, Vol. 275, 2020, pp. 116322.

[10] Liu, Y., Sun, Q., Wang, H., and et al., Effect of the Axial External Magnetic Field on Copper/Aluminium Arc Weld Joining, Science and Technology of Welding and Joining, Vol. 21, No. 6, 2016, pp. 460-465.

[11] Sun, Q., Li, J., Liu, Y., and et al., Arc Characteristics and Droplet Transfer Process in CMT Welding with a Magnetic Field, Journal of Manufacturing Processes, Vol. 32, 2018, pp. 48-56.

[12] Cao, L., Zhou, Q., Liu, H., and et al., Mechanism Investigation of the Influence of the Magnetic Field on the Molten Pool Behavior During Laser Welding of Aluminum Alloy, International Journal of Heat and Mass Transfer, Vol. 162, 2020, pp. 120390.

[13] Chen, R., Kong, H., Luan, J., and et al., Effect of External Applied Magnetic Field on Microstructures and Mechanical Properties of Laser Welding Joint of Medium-Mn Nanostructured Steel, Materials Science and Engineering: A., Vol. 792, 2020, pp. 139787.

[14] Sajed, M., Seyedkashi, S. M. H., Solid-State Local Micro-Alloying of Thick St37 Steel Plates with SiC Powder Using a Modified Friction Hydro-Pillar Process, Journal of Materials Research and Technology, Vol. 9, No. 4, 2020, pp. 7158-7171.

[15] Sajed, M., Seyedkashi, S. M. H., Multilayer Friction Stir Plug Welding: a Novel Solid-State Method to Repair Cracks and Voids in Thick Aluminum Plates, CIRP Journal of Manufacturing Science and Technology, Vol. 31, 2020, pp. 467-477.

[16] Yabuuchi, K., Tsuda, N., Kimura, A., and et al., Effects of Tool Rotation Speed on the Mechanical Properties and Microstructure of Friction Stir Welded ODS Steel, Materials Science and Engineering: A., Vol. 595, 2014, pp. 291-296.

[17] Das, H., Mondal, M., Hong, S. T., and et al., Microstructure and Mechanical Properties Evaluation of Friction Stir Welded Boron Steel, Journal of Mechanical Science and Technology, Vol. 34, 2020, pp. 2011-2017.

[18] Shafique, J., Alrobei, H., and Wakeel, A., et al., Structural and Mechanical Properties of Friction Stir Welded Al2O3 and SiC Reinforced Al 7075 Alloys, Journal of Mechanical Science and Technology, Vol. 33, 2021, pp. 1437-1444.

[19] Zohoor, M., Givi, M. B., and Salami, P., Effect of Processing Parameters on Fabrication of Al–Mg/Cu Composites via Friction Stir Processing, Materials and Design, Vol. 39, 2012, pp. 358-365.

[20] Babu, S. D. D., Sevvel, P., and Kumar, R. S., Simulation of Heat Transfer and Analysis of Impact of Tool Pin Geometry and Tool Speed During Friction Stir Welding of AZ80A Mg Alloy Plates, Journal of Mechanical Science and Technology, Vol. 34, 2020, pp. 4239-4250.